ELSEVIER

Biochimica et Biophysica Acta 1609 (2003) 45–54

BIOCHIMICA ET BIOPHYSICA ACTA
BBA

www.bba-direct.com

Membrane structure of the human immunodeficiency virus gp41 fusion peptide by molecular dynamics simulation II. The glycine mutants

Tuck C. Wong *

Department of Chemistry, University of Missouri, 125 Chemistry Building, Columbia, MO 65211, USA

Received 13 August 2002; received in revised form 25 October 2002; accepted 28 October 2002

Abstract

In this work, molecular dynamics (MD) simulation of the interaction of three mutants, G3V, G5V and G10V, of the human immunodeficiency virus (HIV) gp41 16-residue fusion peptide (FP) with an explicit palmitoyloleoylphosphatidyl-ethanolamine (POPE) lipid bilayer was performed. The goals of this work are to study the correlation of the fusogenic activity of the FPs with the mode of their interaction with the bilayer and to examine the roles of the many glycine residues in the FP in the fusion process. The results of this work corroborate the main conclusion of our earlier MD work of the WT FP and several mutants with polar substitution. These two studies provide correlation between the mode of insertion and the fusogenic activity of these peptides and support the hypothesis that an oblique insertion of the fusion domain of the viral protein is required for fusogenic activity. Inactive mutants interact with the bilayer by a surface-binding mode. The results of this work, combined with the results of our earlier work, show that, while the secondary structures of the wild-type FP and its mutants do not affect the fusogenic activities, the conformational flexibility appears to be an important factor. The active WT FP and its partially active mutants, G3V and G5V, all have significant conformational transitions at one of the glycine sites. They occur at Gly^{5} in **FP-wt**, at Gly^{10} in **FP-G5V** and at Gly^{13} in **FP-G3V**. Thus, a glycine site in each of these active (or partially active) FPs provides conformational flexibility. On the other hand, the inactive mutants **FP-G10V**, **FP-L9R** and **FP-V2E** do not have any conformational transitions except at either terminus and thus possess no conformational flexibility. Thus, the results of this work support the suggestion that the role of glycine residues in the fusion domain is to provide the necessary conformational flexibility for fusion activity.

The glycines also form a ''glycine strip'' in the FP that locates on one (the less hydrophobic) face of the helix (the ''sided helix''). However, whether this ''glycine strip'' is disrupted or not does not seem to correlate with the retention of fusogenic activities. Finally, although the FLGFL (8–12) motif is absolutely conserved in the HIV fusion domain, a well-structured motif stabilized by hydrogen bonding does not appear to be required for activity. In fact, hydrogen bonding in this motif was found to be missing in **FP-G3V** and **FP-G5V**. Both of these mutants are partially active.

Keywords: Fusion peptide; Glycine mutant; Molecular dynamics simulation

1. Introduction

Enveloped viruses such as human immunodeficiency virus (HIV) and influenza virus infect their target cells by cell-specific binding to the cell membrane followed by the fusion of the viral enveloped membrane with cellular membranes [1]. Usually, only one viral protein is responsible for the actual membrane fusion step. For many viruses, a segment of the fusion protein usually located at the N-terminus of the fusion protein is responsible for the initial stage in the membrane fusion process [2]. This segment is generally referred to as the fusion domain or fusion peptide (FP). The interaction of the FP with membranes has many membrane perturbing properties [3] and accelerates the rate of liposome fusion in model membrane systems. The HIV-1 fusion protein, glycoprotein gp160, contains two noncovalently associated subunits, gp120 and gp41 [1]. The subunit gp120 contains sites for viral binding to target cells containing CD4 [4] and chemokine receptors [5–7], while the transmembrane subunit, gp41, is responsible for the mem-

* Tel.: +1-573-882-7725; fax: +1-573-882-2754.
E-mail address: wongt@Missouri.edu (T.C. Wong).

0005-2736/02/$ - see front matter © 2002 Elsevier Science B.V. All rights reserved.
PII: S0005-2736(02)00652-1

brane fusion process [8]. The N-terminal 16 residues of the gp41 fusion domain (AVGIGALFLGFLGAAG) are mostly hydrophobic, while the extended domain containing 23 or 33 residues contains more polar residues. The FP is highly homologous with corresponding domains of other enveloped viruses [9]. An absolutely conserved five-residue FLGFL sequence at positions 8–12 is a prominent motif among the HIV family, and was proposed to be essential in fusogenic activities [10].

Mutagenesis studies of intact enveloped proteins as well as the synthetic FPs strongly implicated the role of the FP domain in mediating membrane fusion [11–13]. Mutations with a polar residue in this domain either in intact gp41 fusion protein or in synthetic peptides, such as V2E and L9R, reduce the fusogenic activities drastically [12–14]. The fusion domains of HIV-1 and many other enveloped viruses such as HIV-2, SIV and influenza contain an unusually large number of glycine residues. When the FP is in an α-helical structure, it was proposed that the glycines are located on one face of the helix (the glycine strip) facing the aqueous phase [15], a situation similar to the transmembrane domains of class II MHC molecules [16]. Mutation study involving systematically substituting the glycine residues with the more hydrophobic and bulky valine showed that these mutations either reduce or eliminate the activity of the FP [13]. When the glycines at position 10 and 13 in the absolutely conserved FLGFLG motif are mutated, the activity was found to be completely eliminated. Mutations of the glycines at position 3 and 5 reduce but do not eliminate the activity of the FP. The conservation of these glycine residues and the aforementioned mutational study [13] strongly suggests their special role in the fusion process. However, despite speculations, the exact roles of these glycine residues have not been determined.

Polarized attenuated total reflection infrared spectroscopy (ATR-IR) has been used to determine the orientation of FPs with respect to the membrane surface [17,18]. It was suggested that, based on the correlation of the tilt angle of the inserted FP with respect to the membrane interface and the fusogenic activity of the FP, the oblique insertion of the viral FP is required for fusogenic activities. Inactive FP mutants orient parallel or more parallel to the membrane surface instead. Results from NMR [19] and ESR power saturation techniques [20,21] for the influenza HA2 FP also reached such a conclusion.

To date, only a few modeling/simulation studies on the interaction of viral FPs with membrane have been carried out. Hydrophobic moments and hydrophobic index have been used to estimate the interaction of the HIV and other FP's with membrane. Efremov et al. [22] used Monte Carlo simulation to study the orientation of the influenza hemagglutinin HA_2 (1–20) FP in a lipid bilayer represented by a two-phase slab model. Bechor and Ben-Tal [23] used molecular dynamics (MD) in an implicit solvent model to study the orientation of the same FP with respect to the membrane and found that the lowest free energy configuration of the system is the parallel (between the peptide helical axis and the membrane-water interface) orientation rather than the oblique orientation suggested from experimental results [19,24]. The authors attributed the discrepancy to the lack of head group–peptide interaction and the lack of peptide-induced membrane deformation in the implicit solvent model. Recently, we reported the first MD simulation study of the HIV-1 FP in an *explicit* palmitoyloleoylphosphatidyl-ethanolamine (POPE) lipid bilayer, in which the wild-type FP, its V2E and L9R mutants and a shortened peptide consisting of the 5–16 segment were studied. The results showed that the active WT peptide is inserted into the bilayer at $\sim 45^\circ$, while the inactive mutants and fragment bind to the surface of the bilayer and lie parallel to the bilayer surface [25]. Thus, it demonstrated that MD in explicit membrane model can produce results that are consistent with experiments. The MD results are in agreement with the hypothesis that in order for the FP to be active, it must be inserted into the bilayer in an oblique angle.

In this work, three mutants of the 16-residue FP of the HIV-1 gp41 protein involving substituting glycine residues in three different locations with a more hydrophobic and bulky residue valine, G3V, G5V and G10V (hereafter referred to collectively as the G-mutants), were studied by MD simulation in an explicit POPE bilayer. POPE bilayer was used because previous work [17] showed that the WT FP can only cause fusion in large unilamllar vesicles when PE is present and that the orientation of the FP with respect to the bilayer surface depends on the presence of PE. The purpose of this work is to test the hypothesis that in order for the FP to be active, it must be inserted into the bilayer in an oblique angle, and to determine the roles the many glycine residues in the FP play in the membrane interaction and fusion process.

2. Methods

The explicit peptide–POPE bilayer in water was subjected to MD simulations and minimizations using NAMD [26] version 2.4 running on a dual processor Linux system. The all-atom CHARMM PARAM-27 force field was used for the peptides [27] and lipids [28]. The nonbonded list was generated using a group-based cutoff of 14.0 Å. The van der Waals (vdW) interactions were smoothly switched from 10.0 to 12.0 Å. The long-range electrostatic interactions were handled by the particle mesh Ewald (PME) algorithm [29] using a $48 \times 48 \times 81$ grid and a β-spline interpolation of 4th order. All the peptides were constructed in an α-helical conformation. The N-terminus was protonated and the C-terminus was modeled as a carboxamide. The coordinates for the POPE system were obtained from Professor Helmut Heller's laboratory (http://www.lrz-muenchen.de/~heller/membrane/membrane.html) and a bilayer slice of 50×50 Å from the center of the bilayer system was used for simulation. The procedure for making the initial POPE

bilayer is as reported in our previous work [25]. The peptide was next inserted into the upper leaflet of the bilayer keeping the helical axis perpendicular to the bilayer surface. The POPE and water molecules overlapping with the peptide were deleted. The final bilayer had 33 and 40 lipid molecules on the upper and lower leaflets of the bilayer, respectively. The SHAKE algorithm [30] was used to fix the lengths of bonds involving hydrogen atoms. The Newton's equations of motion were integrated every 2 fs using the MTS Impulse-Verlet (r-RESPA) algorithm. Full electrostatics integration was done every step. Periodic boundary conditions were applied to the system to prevent distortions at the boundary of the system as a result of exposure to vacuum. The system was minimized for 2000 cycles using steepest descents to remove bad vdW contacts. The system was then heated in steps of 25 K every 0.2 ps until it reached the simulation temperature of 320 K. Following heating, the temperature was reassigned to 320 K every 0.2 ps for another 20 ps. The temperature of the system was then maintained at 320 K during the entire data sampling period. The nonbonded list was updated every 10 steps. A NPT ensemble was used during data sampling. The collision frequency of the Langevin piston was set to 25 ps^{-1} and the mass of the piston to 500 amu [31]. The pressure was maintained by changing the box length in the *Z*-direction along the bilayer axis. The surface area was kept constant. During this stage, the trajectory was sampled every 0.5 ps. The total simulation time was 2.0 ns for each FP.

3. Results

3.1. The insertion of the fusion domain

Since the peptides maintained their helical nature over a major part of the sequence during the entire simulation (see discussion later), the orientation of the peptides was measured by the tilt angle of the helical axis of the peptides with respect to the bilayer normal. The time evolution of the tilt angle of the helical axis for the three mutants, G3V, G5V and G10V, are compared with that of the wild-type peptide previously studied in the same POPE bilayer [25]. In the initial configuration of all these peptides, the helical axis was oriented parallel to the bilayer normal (i.e. perpendicular to the bilayer surface). The helical axis slowly tilted during the simulation in each case. For **FP-wt**, the helical axis reached an equilibrium orientation of $44 \pm 6°$ with respect to the bilayer normal from $\sim$ 300 ps on Ref. [25]. Significant changes in the helical axis orientation from that of **FT-wt** were seen following the mutations. The mutants **FP-G3V** and **FP-G10V**, oriented at $92 \pm 17°$ and $82 \pm 16°$ with respect to the bilayer normal, respectively, after reaching their equilibrium configurations. The structure of **FP-G5V**, on the other hand, consists of two helical segments, the 4–9 and 11–16 segments, orienting differently with respect to the bilayer normal, with Gly^{10} acting as a hinge. The tilt angles for these two segments were found to be $110 \pm 18°$ and $82 \pm 16°$, respectively. Thus, the 11–16 segment lies essentially parallel to the interface, while the 4–9 segment evolved into an orientation in which the N-terminus protrudes towards the membrane/aqueous interface. Larger fluctuations were observed in these mutants which emerged onto the surface of the bilayer than for the wild-type FP that was inserted [25]. In particular, the 4–9 segment of **FP-G5V** experiences large fluctuations that change the orientation of this segment from protruding towards the aqueous phase to pointing towards the bilayer interior (Fig. 1). The implication of the results in this work is in good agreement with our earlier work on the HIV FP, its mutants with polar substitutions and a shortened peptide [25] in that the results support the hypothesis that active FP inserts into the membrane at an oblique angle while inactive and partially active mutants either bind onto the surface of the membrane or insert only shallowly. The orientational data do not provide differentiation between the completely inactive G10V and the partially active G3V and G5V mutants [13]. Overall, the conclusion from this work is in support of the hypothesis linking oblique insertion to fusogenic activities.

The gross position of the FPs in the lipid bilayer and its location relative to the various components of the phospholipids and water are illustrated in Fig. 2 for **FP-G10V**. The positions of the side chains and backbones of the various residues in the peptides in the POPE bilayer provide information on the extent of the insertion of the various peptides into and the interaction of the various groups of the peptide with the bilayer. In Fig. 3, the locations of the backbone and the side chains (average positions of the heavy atoms on the backbone and the side chain, respectively) of the peptides in the POPE matrix are shown. The interfacial area of the bilayer between the lipids and water is defined by the positions where the hydrocarbon and water densities pass through 10% of their respective bulk values [32]. The interfacial area in each system in Fig. 3 is indicated by the two horizontal lines. The phosphate and ethanolamine groups are distributed in the head group area that is 2–3 Å closer to the aqueous phase than the interfacial area (Fig. 2). **FP-wt** has its N-terminal segment inserted deeper than the interfacial area while the C-terminal segment lies in the head group area. The G3V mutation causes the peptide to lie entirely in the interfacial and head group areas. There is a change of the orientations of 2–3 segment. With the substitution of Val in position 3, the hydrophobic Val^2 is forced to rotate towards the aqueous phase, allowing Val^3 and Ile^4 to face the hydrophobic interior of the bilayer. In addition, the side-chains of Leu^7 and Phe^{11} protrude into the hydrophobic core. The "glycine strip" [13,14] observed in **FP-wt** in our previous MD simulation [25], however, is completely maintained, because even in **FP-wt**, Gly^3 is on the more hydrophobic face of the helix and is not part of this glycine strip. Similarly, for **FP-G10V**, the side-chains of Ile^4, Leu^7 and Phe^{11} are most responsible for the

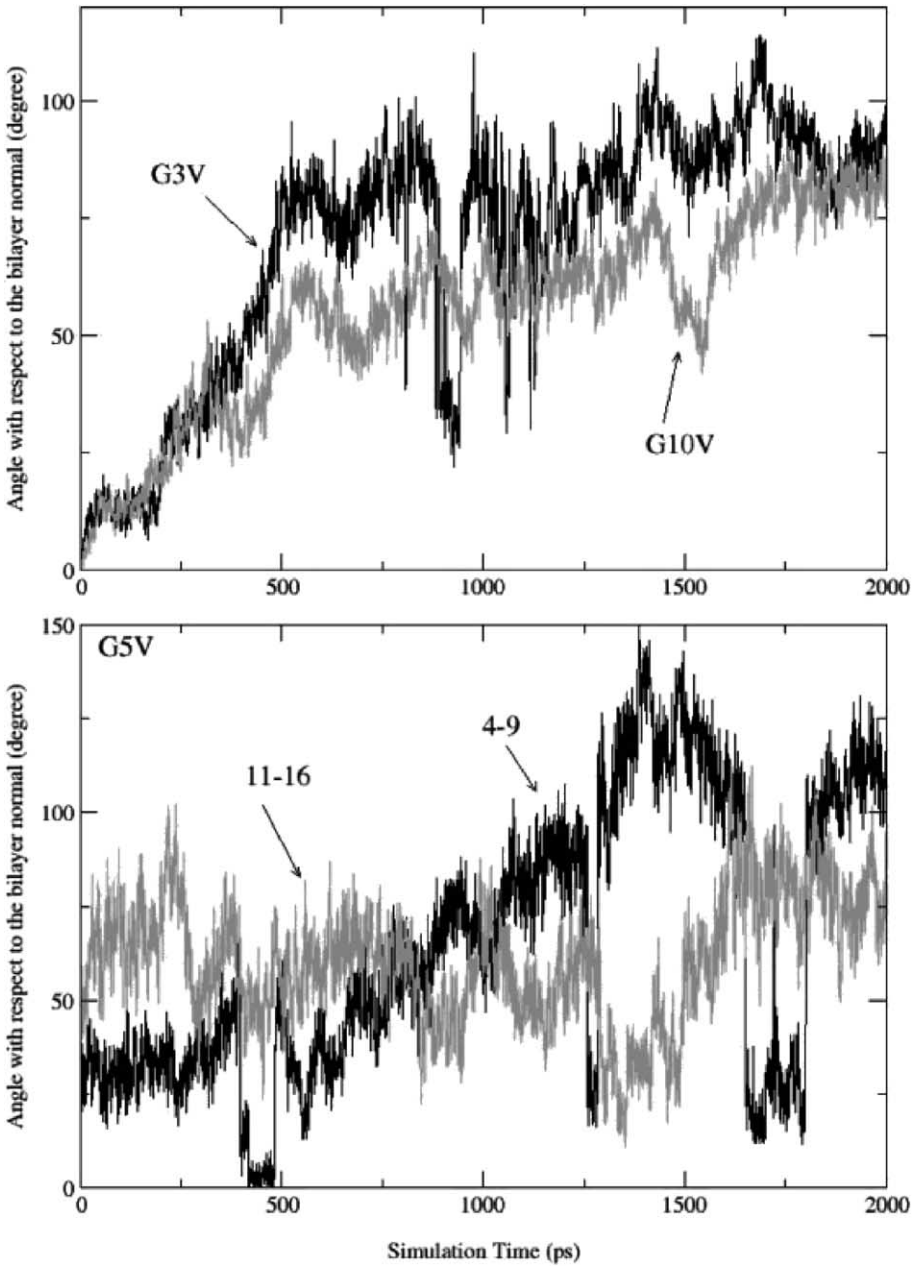

Fig. 1. The time-evolution of the orientation of the helical axis with respect to the normal to the POPE bilayer for **FP-G3V**, **FP-G10V** and the two helical components of **FP-G5V**. For comparison, the average orientation for **FP-wt** as determined by MD was $44 \pm 6°$ [25].

interaction of the hydrophobic core of the bilayer. For **FP-G5V**, the N-terminal segment is more exposed to the aqueous phase. The Val substitution at position 5 actually causes Ile^4 to insert less deeply into the bilayer than in **FP-wt**. Thus, the side chains of Leu^7, Phe^8, Phe^{11} and Leu^{12} may account for most of the hydrophobic interactions of the peptide with the bilayer. In both **FP-G5V** and **FP-G10V**, with the Val residue (at positions 5 and 10, respectively) on the less hydrophobic face of the helix, the glycine strip and the "sided-helix" [15] properties, were partially disrupted by the replacement of the glycine residue at positions 5 and 10, respectively.

3.2. The conformation and conformational transitions

FP-wt and the three mutants studied maintained their helical structure over a major portion of the peptide throughout the simulations. The helical region extends from 3 to 15 in **FP-G3V**, and from 4 to 15 for **FP-G10V**. **FP-G5V**, however, consists of two helical segments, the 4–9 and 11–16 segments, with Gly^{10} acting as a hinge between these two helices. The angle between the two helical segments varied over a wide range during the 2-ns simulation. Several previous work has indicated that the conformation of the FPs is mostly helical under the condition of low peptide loading (peptide/

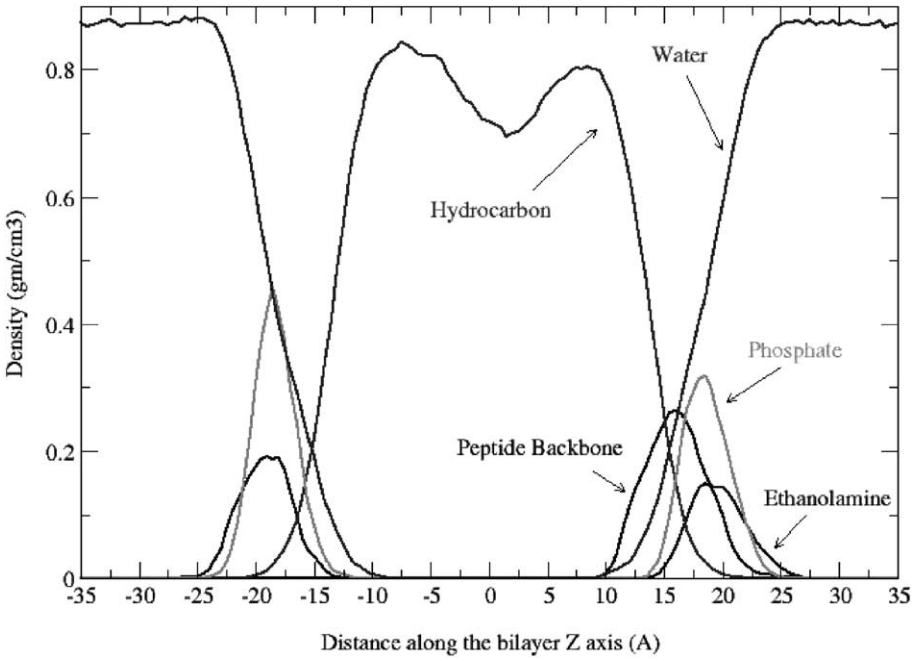

Fig. 2. The distribution of the densities of the backbone of the peptide **FP-G10V**, the lipid hydrocarbon chains, choline and phosphate groups along with water in the **FP-G10V**/POPE bilayer system.

lipid ratio) [33,34]. A recent work using ^{13}C-enhanced FTIR [35] showed that the α-helical segment for the WT FP start from Gly^{5} and extends to Ala^{15} in various membrane mimicking media. NMR work of the WT FP in sodium dodecylsulfate micelles also revealed the same helical region [36].

For the most part, the ϕ, ψ angles of each corresponding residues of these peptides are similar and there are no major differences between the secondary structures of the active **FP-wt**, and the less active or inactive **FP-G3V**, **FP-G5V** and **FP-G10V** (Table 1). This result supports the suggestion that the variation in the secondary structure in the fusion domain plays little or no role in their fusogenic activities [34,37,18,25]. However, the conformational flexibility of the FPs seems to have significant bearings on their fusogenic activities as will be discussed in the next section.

The hydrogen bonding patterns in these three mutants have been analyzed from their MD trajectories. The criteria for defining a hydrogen bond are an average acceptor (the carbonyl oxygen in this case)-hydrogen distance of <2.8 Å and an average O–H–N angle of $>120°$ [38]. Hydrogen bonding patterns characteristic of an α-helix, i.e., C=O (*i*)-NH (*i*+4), and some C=O (*i*)-NH (*i*+3), hydrogen bonds, with the *i*, *i*+4 hydrogen bonds being usually the stronger as judged by the shorter distance between the O and H atoms and the larger O...H–N angle, are observed through most part of all four of the peptides, indicating an α-helical structure. The exceptions are in the region from Leu^{7} to Phe^{11} for **FP-G5V** and from Leu^{9} to Phe^{11} for **FP-G3V**, where the *i*, *i*+3 and *i*, *i*+4 hydrogen bonds with the amide protons are missing (or are much weaker) (Table 2). This break in hydrogen bonding is similar to the **FP-wt** case where the *i*, *i*+3 and *i*, *i*+4 hydrogen bonds are missing from Ile^{4} to Leu^{7} [5]. The Gly to Val mutation clearly increases the overall hydrophobicity of the mutants and may increase the α-helical propensity. The latter effect can be seen most clearly in G10V where the α-helical structure is more prevalent than the WT and other G-mutants (Table 2). Yet, it is the least active among this group of FPs. Thus, an increase in α-helical propensity is not correlated with increased fusogenic activities.

The loss of hydrogen bonding described above is accompanied by increased conformational flexibility in the affected region. It appears from this work and from our earlier MD work [25] that higher conformational flexibility, in the form of conformational transitions as well as larger root mean square (rms) variations in the $\phi - \psi$ angles of the relevant residues (Table 1), is exhibited by the active **FP-wt**, and the partially active G5V and G3V mutants. The conformational transitions center at Gly^{5} in **FP-wt**, at Gly^{10} in **FP-G5V** and at Gly^{13} in **FP-G3V** (Fig. 4). In addition to **FP-G5V**, where the transitions take place at Gly^{10} as described earlier, in **FP-G3V**, there are concerted transitions for $\phi(13)$ and $\psi(12)$ at 1.2 ns during the 2-ns simulation (Fig. 4). This conformational transition persisted for about 400 ps and the peptide returned to the original conformation, causing the peptide to go from a linear to a V-shaped form. Our previous work [25] showed that the transitions for **FP-wt** occurred at the phi angle of Ala^{6} (and at Gly^{3} and Leu^{9}) and psi angle of Gly^{5} leading the peptide to go from a linear to a V-shaped form pivoted at Gly^{5}. Studies of the influenza HA FP also showed similar hinge type of conformation [21]. In contrast, there is little conformational flexibility in the inactive G10V mutant

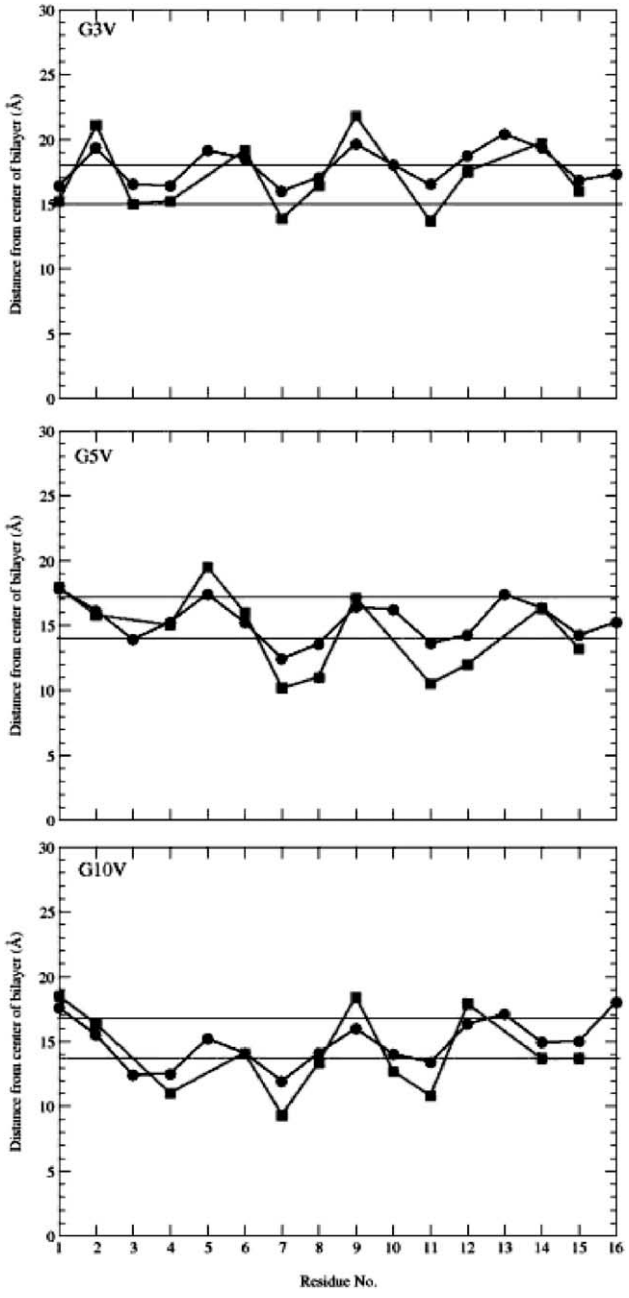

Fig. 3. The distribution of the peptide backbone (●) and side chains (■) of each residue in **FP-G3V**, **FP-G5V** and **FP-G10V** with respect to the interfacial region of the POPE bilayer system (indicated by the two horizontal lines in each figure). A similar plot for **FP-WT** was given in Ref. [25]. Note that these figures have not been drawn to reflect the angle of orientation with respect to the bilayer accurately.

as shown in this study and in the inactive V2E mutant in our earlier work [25]. In both cases, the hydrogen bond network extends throughout the peptide (Table 2 and Ref. [25]). Analysis of the interaction between the C=O oxygen and the N–H proton of the peptide backbone with water via the respective RDF provided corroborative information on the intermolecular hydrogen bonding in these peptides. The C=O from C-terminal residues 13–16 in each FP are all well hydrated because they are not involved in the (i, $i+3$), or (i, $i+4$) intramolecular hydrogen bonding. For the rest of the peptides, the RDFs showed that the carbonyl oxygen atoms of Leu^{9}, Gly^{10}, Leu^{12} and, to a lesser extent, of Gly^{5} and Ala^{6}, in **FP-G3V** are hydrated by water. Similarly, in **FP-G5V**, the carbonyls of residues Leu^{7}–Leu^{12} are strongly hydrated. This partially accounts for (or is the result of) the weakening or breaking of the hydrogen bonding in these respective segments. In contrast, the carbonyls of only the C-terminal segment 12–16 in **FP-G10V** were found to be significantly hydrated as described above because of the uninterrupted hydrogen bonding pattern in the 4–15 segment in this peptide.

The strongest hydrogen bonds were found in the FLGFL (8–12) motif and extending towards the C-terminus for **FP-wt** and for the V2E and L9R mutants [25]. This is also the case for the inactive **FP-G10V** from the present study (Table 2). However, hydrogen bonding in this motif was found to be largely or completely missing in **FP-G3V** and in **FP-G5V**, both of which possess partial fusogenic activity. Thus, having a well-structured FLGFL motif stabilized by hydrogen bonding does not seem to be an essential structural feature for fusogenic activities, despite the absolute conservation of this motif in various HIV-1 strains.

3.3. Peptide hydration and peptide–head group interactions

In the previous section, the hydration of the C=O groups in the mid-section of the peptide in relation to the existence or the lack of intramolecular hydrogen bonds was discussed. The C=O of the C-terminal segment of these peptides are also more hydrated, indicating greater exposure to the aqueous phase consistent with the insertion pattern and the locations of the C-terminal segment with respect to the membrane–water interface.

The N-terminal peptide bond of these mutants, as is in **FP-wt**, is not significantly exposed to the hydrophobic environment because Ala^{1} is either oriented upward towards the interfacial area, as is the N-terminus in influenza HA_2 FP [19,20], or is located in the interfacial area. Instead, the NH_3^+ group of Ala^{1} of these peptides is significantly hydrated and it has strong interactions with the phosphate head groups of POPE. This indicates that the N-terminus is close to the interfacial area and the favorable interactions with the negatively charged part of the head groups provide stabilization of such a configuration. The role of the latter interaction in stabilizing the configuration of the FP in the membrane was also speculated in the study of Macosko et al. [20] in their study of the influenza HA_2 FP. This interaction and the reluctance of the protonated N-terminus to be exposed to the hydrophobic bilayer interior are the main reasons that the peptides do not insert perpendicularly into the bilayer.

As in our previous study of **FP-wt** and its polar mutants (L9R and V2E), very little interaction between the backbone of the peptides with the phospholipid head groups was

Table 1
ϕ and ψ values (in degrees) for the wild-type fusion peptide and its mutants in a POPE bilayer

Residue	Phi and psi values[a]							
	FP-WT		**FP-G3V**		**FP-G5V**		**FP-G10V**	
	ϕ	ψ	ϕ	ψ	ϕ	ψ	ϕ	ψ
2	−85 ± 18	132 ± 14	−94 ± 14	86 ± 14	−98 ± 22	168 ± 13	−110 ± 14	129 ± 17
3	102 ± 22	−13 ± 24	−68 ± 10	−55 ± 15	70 ± 16	−113 ± 23	−63 ± 19	−107 ± 19
4	−72 ± 14	−57 ± 10	−65 ± 12	−36 ± 13	−73 ± 10	−27 ± 11	−69 ± 9	−39 ± 9
5	**−62 ± 22**	**−18 ± 36**	−65 ± 11	−36 ± 15	−72 ± 10	−45 ± 9	−64 ± 10	−31 ± 11
6	**−96 ± 31**	−63 ± 13	−69 ± 13	−44 ± 13	−60 ± 10	−42 ± 10	−70 ± 10	−43 ± 9
7	−90 ± 15	−54 ± 12	−72 ± 12	−49 ± 13	−61 ± 10	−38 ± 12	−61 ± 10	−42 ± 9
8	−75 ± 12	−34 ± 12	−66 ± 12	−54 ± 10	−75 ± 13	−52 ± 11	−63 ± 10	−43 ± 10
9	−47 ± 19	−44 ± 16	−70 ± 10	−27 ± 13	−78 ± 13	**−44 ± 24**	−62 ± 10	−39 ± 9
10	−65 ± 11	−35 ± 12	−66 ± 12	−38 ± 13	**−130 ± 29**	**44 ± 39**	−64 ± 9	−40 ± 10
11	−74 ± 11	−39 ± 9	−70 ± 11	−51 ± 11	**−88 ± 24**	−51 ± 12	−64 ± 10	−51 ± 9
12	−65 ± 9	−40 ± 10	−66 ± 14	**−6 ± 64**	−63 ± 13	−48 ± 14	−66 ± 10	−32 ± 13
13	−67 ± 11	−30 ± 15	**−25 ± 91**	**−41 ± 23**	−77 ± 15	−31 ± 20	−72 ± 13	−31 ± 17
14	−72 ± 12	−37 ± 12	−80 ± 15	−51 ± 14	−78 ± 15	−48 ± 14	−81 ± 14	−47 ± 15
15	−73 ± 12	−55 ± 17	−77 ± 13	−51 ± 38	−74 ± 12	−36 ± 45	−78 ± 15	−42 ± 80

The dihedral angles with large rms deviations due to conformational transitions (not including those at or close to the termini) are depicted in bold.
[a] Values are reported as average ± rms deviations.

found in these three mutants, nor was there any significant interactions between the mostly hydrophobic side chains and the lipid head groups. By examining the RDFs between the C=O groups of the peptide backbone and ethanolamine groups on the lipid and between the amide protons on the peptides and the phosphate groups on the lipids, nonnegligible interactions were found only between the N-terminal C=O with the amine groups in the ethanolamine head groups in **FP-G3V**, and the C=O groups of Ala[15] and Gly[16] in **FP-G10V**. An exception was found in **FP-G5V**. Since the middle (Leu[7]–Phe[11]) part of this peptide lacks intramolecular hydrogen bonds, the C=O of Leu[9] was also found to interact rather strongly with the ethanolamine head groups. Interactions between the amide protons on the backbone of the peptide with the phosphate head groups were not observed except for both terminal residues in **FP-G10V** and for the N-terminal residues for the other two mutants. Since the N-terminal segment of **FP-G5V** protrudes towards the aqueous phase, the interaction of the Ala[1] amino group of **FP-G5V** with the phosphate head groups was weaker than the other two mutants, while the hydration of the N-terminal amino group was stronger. Based on the lack of interactions of either the backbone or the side chains of the gp41 FPs with the lipid head groups and based on the positions of the hydrophobic side chains (primarily of Ile[4], Leu[7], Phe[8], Phe[11] and Leu[12]), it can be inferred that the interaction of the FPs with the bilayer is primarily through the hydrophobic side chains.

Table 2
Hydrogen bonding patterns for the wild-type fusion peptide and its mutants

H-bond pattern	Bond angles and bond distances[a]							
	FP-WT		**FP-G3V**		**FP-G5V**		**FP-G10V**	
	Angle	Distance	Angle	Distance	Angle	Distance	Angle	Distance
2 → 5							126 ± 14	2.49 ± 0.4
2 → 6	–	–	–	–	–	–	141 ± 14	2.69 ± 0.4
3 → 6							127 ± 14	2.69 ± 0.3
3 → 7	145 ± 16	2.86 ± 1.0	158 ± 12	2.34 ± 0.4	158 ± 12	2.18 ± 0.3	152 ± 13	2.43 ± 0.4
4 → 8	–	–	152 ± 17	2.21 ± 0.4	146 ± 16	2.50 ± 0.4	158 ± 11	2.25 ± 0.3
5 → 8					122 ± 14	2.68 ± 0.4		
5 → 9	–	–	139 ± 27	2.69 ± 0.8	163 ± 10	2.00 ± 0.2	157 ± 11	2.15 ± 0.3
6 → 10	–	–	129 ± 17	2.69 ± 0.5	144 ± 20	2.26 ± 0.4	162 ± 10	2.05 ± 0.2
7 → 11	–	–	146 ± 16	2.43 ± 0.5	–	–	154 ± 12	2.66 ± 0.4
8 → 11	126 ± 16	2.44 ± 0.3	123 ± 15	2.69 ± 0.4	–	–	–	–
8 → 12	159 ± 12	2.11 ± 0.3	161 ± 11	2.11 ± 0.3	–	–	161 ± 10	2.12 ± 0.2
9 → 13	154 ± 14	2.10 ± 0.3	–	–	–	–	158 ± 11	1.95 ± 0.2
10 → 14	141 ± 18	2.48 ± 0.5	–	–	–	–	143 ± 18	2.42 ± 0.4
11 → 14	–	–	–	–	–	–	123 ± 14	2.76 ± 0.4
11 → 15	149 ± 16	2.31 ± 0.4	139 ± 25	2.54 ± 0.7	149 ± 23	2.34 ± 0.6	157 ± 14	2.06 ± 0.3
12 → 16	154 ± 21	2.16 ± 0.5	–	–	135 ± 32	2.76 ± 1.1	135 ± 26	2.43 ± 0.6

[a] Bond angle is the O...H–N angle in degrees and the bond distance is the O...H distance in Å. Values are reported as average ± rms deviations.

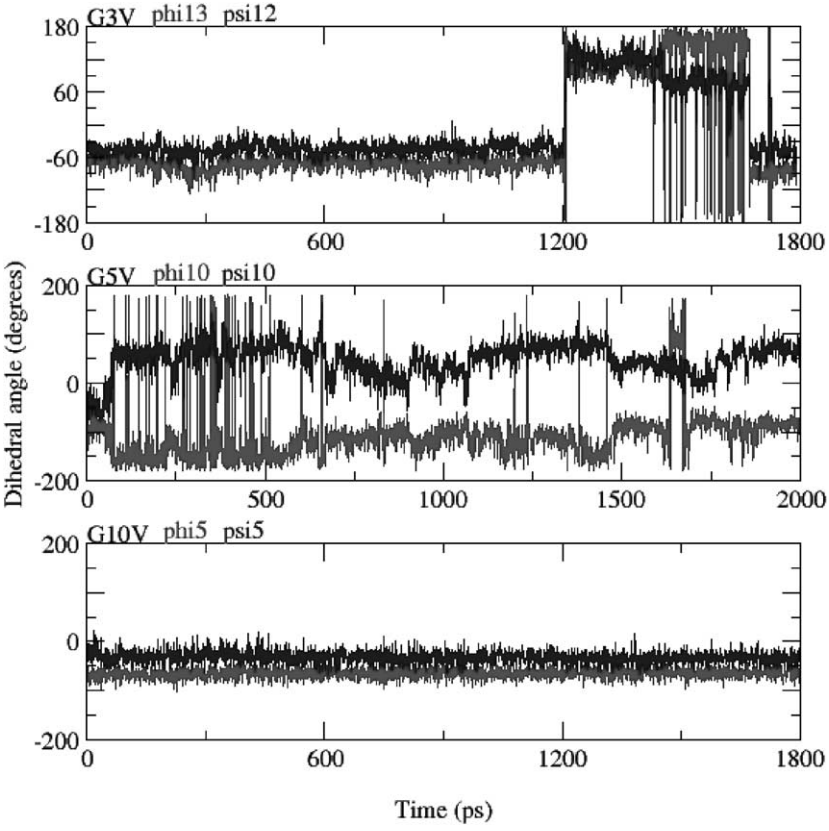

Fig. 4. The conformational transitions for **FP-G3V** at Leu[12] and Gly[13] and for **FP-G5V** at Gly[5]. The ϕ, ψ angles vs. time plot for Gly[5] of **FP-G10V** is also presented for comparison. No such transition at Gly[5] or at any other residues was observed for the inactive **FP-G10V** except at Ala[15] near the C-terminus.

3.4. The perturbation of the bilayer

In our earlier work [25], it was shown that the insertion of FP-wt perturbed the bilayer order by increasing the length of the interfacial area by ~ 1.2 Å, while the inactive mutants did not. The increase of the interfacial area has been shown to be due to the disorientation of the lipid that extends the lipid density towards the head group region, rather than due to increased water penetration. In this work, it was shown that the interaction of these three G-mutants with the bilayer produced negligible perturbation of the bilayer. In all three systems, the length of the interfacial area in the upper leaflet was found to be essentially the same as that of the lower leaflet. In both leaflets, the interfacial area thickness was 3.0 ± 0.2 Å. The results here showed that surface binding or shallow insertion of the FP does not produce observable perturbation of the membrane.

4. Conclusions

In this work, the results of an explicit MD study of the interaction of three mutants of the HIV gp41 16-residue fusion domain with a POPE lipid bilayer were presented. The results of this work corroborate the main conclusion of our earlier MD work of the WT FP and several mutants with polar substitutions. These two studies provide correlation between the mode of insertion and the fusogenic activity of these peptides and support the hypothesis that an oblique insertion of the fusion domain of the viral protein is required for fusogenic activity [18,39]. Inactive mutants interact with the bilayer by a surface-binding mode. One objective of this work is to examine the roles of the many glycine residues in the fusion domain. This work, when combined with the result of our earlier work, showed that while the (mostly helical) secondary structures of the wild-type FP and its mutants do not affect the fusogenic activities, the conformational flexibility does appear to be an important factor. The active WT FP and its partially active mutants, G3V and G5V, all have significant conformational transitions at a glycine site. They occur at Gly[5] in **FP-wt** (see Fig. 5 in Ref. [25]), at Gly[10] in **FP-G5V** and at Gly[13] in **FP-G3V** (Fig. 4). Thus, a glycine site in each of these active (or partially active) FPs provides conformational flexibility. On the other hand, the inactive mutants **FP-G10V**, **FP-L9R** and **FP-V2E** do not have any conformational transitions except at either terminus (for example at Ala[15] for **FP-G10V**) and thus possess no conformational flexibility. Thus, the results of this work suggest that one of the important roles of glycine residues in the fusion domain is to provide the necessary conformational flexibility for fusion activity. Previous work on the gp41 FP revealed the controversies on whether the

FP adopts an α-helical or β structure. Even experiments under similar sample conditions have shown both the α and β structures [18,40–43]. It is hypothesized by some groups that conformational polymorphism and/or the ability to convert readily between α-helical and β-conformations of the inserted FP are essential [3,44]. The conformational variability may contribute to the flexibility of the fusogenic complex during the membrane fusion process [45–47], and/or allowing access of the FP to the trans monolayer of the target membrane during membrane fusion [44]. Perhaps the conformational flexibility observed here is needed to facilitate the $\alpha - \beta$ conversion in the FPs or the conformational changes required for the subsequent fusion process.

The glycine residues form a "glycine strip" that locates on one (the less hydrophobic) face of the helix. However, whether this "glycine strip" is disrupted in the G3V and G5V mutants does not seem to correlate with a loss of fusogenic activities. Finally, although the FLGFL (8–12) motif is absolutely conserved in the HIV fusion domain, a well-structured motif stabilized by hydrogen bonding does not appear to be required for activity. In fact, hydrogen bonding in this motif was found to be missing in FP-G3V and FP-G5V, both of which are partially active.

Acknowledgements

Supports by the Petroleum Research Fund, administered by the American Chemical Society (35495-AC7), the University of Missouri Research Board and the Pittsburgh Supercomputing Center are gratefully acknowledged. We thank Dr. S. Kamath for running some of the simulations and analyses.

References

[1] F.D. Veronese, A.L. DeVico, T.D. Copeland, S. Oroszlan, R.C. Gallo, M.G. Sarngadharan, Science 229 (1985) 1402–1405.
[2] D.C. Chan, D. Fass, J.M. Berger, P.S. Kim, Cell 89 (1997) 263–273.
[3] S.G. Peisajovich, R.F. Epand, M. Pritsker, Y. Shai, R.M. Epand, Biochemistry 39 (2000) 1826–1833.
[4] A.L. Lasky, G. Nakamura, D.H. Smith, C. Fennie, C. Shimasaki, E. Patzer, P. Berman, T. Gregory, D.J. Capon, Cell 50 (1987) 975–985.
[5] H. Choe, M. Farzan, Y. Sun, N. Sullivan, B. Rollins, P.D. Ponath, L.J. Wu, C.R. Mackay, G. LaRosa, W. Newman, N. Gerard, C. Gerard, J. Sodroski, Cell 85 (1996) 1135–1148.
[6] B.J. Doranz, J. Rucker, Y.J. Yi, R.J. Smyth, M. Samson, S.C. Peiper, M. Parmentier, R.G. Collman, R.W. Doms, Cell 85 (1996) 1149–1158.
[7] T. Dragic, V. Litwin, G.P. Allaway, S.R. Martin, Y.X. Huang, K.A. Nagashima, C. Cayanan, P.J. Maddon, R.A. Koup, J.P. Moore, W.A. Paxton, Nature 381 (1996) 667–673.
[8] M. Kowalski, J. Potz, L. Basiripour, T. Dorfman, W.C. Goh, E. Terwilliger, A. Dayton, C. Rosen, W. Haseltine, J. Sodroski, Science 237 (1987) 1351–1355.
[9] W.H. Gallaher, Cell 50 (1987) 327–328.
[10] M. Pritsker, J. Rucker, T.L. Hoffman, R.W. Doms, Y. Shai, Biochemistry 38 (1999) 11359–11371.
[11] E.O. Freed, D.J. Myers, R. Risser, Proc. Natl. Acad. Sci. U. S. A. 87 (1990) 4650–4654.
[12] E.O. Freed, E.L. Delwart, G.L. Buchschacher, A.T. Panganiban, Proc. Natl. Acad. Sci. U. S. A. 89 (1992) 70–74.
[13] M.D. Delahunty, I. Rhee, E.O. Freed, J.S. Bonifacino, Virology 218 (1996) 94–102.
[14] P.W. Mobley, A.J. Waring, M.A. Sherman, L.M. Gordon, Biochim. Biophys. Acta 1418 (1999) 1–18.
[15] J.M. White, Annu. Rev. Physiol. 52 (1990) 675–697.
[16] P. Cosson, J.S. Bonifacino, Science 258 (1992) 659–662.
[17] I. Martin, F. Defrise-Quertain, E. Decroly, M. Vandenbranden, R. Brasseur, J.M. Ruysschaert, Biochim. Biophys. Acta 1145 (1993) 124–133.
[18] I. Martin, H. Schaal, A. Scheid, J.M. Ruysschaert, J. Virol. 70 (1996) 298–304.
[19] Z. Zhou, J.C. Makosko, D.W. Hughes, B.G. Sayer, J. Hawes, R.M. Epand, Biophys. J. 78 (2000) 2418–2425.
[20] J.C. Macosko, C.H. Kim, Y.K. Shin, J. Mol. Biol. 267 (1997) 1139–1148.
[21] X. Han, J. Bushweller, D. Cafiso, L.K. Tamm, Nat. Struct. Biol. 8 (2001) 715–720.
[22] R.G. Efremov, D.E. Nolde, P.E. Volysky, A.A. Chernyavsky, P.V. Dubovskii, A.S. Arseniev, FEBS Lett. 462 (1999) 205–210.
[23] D. Bechor, N. Ben-Tal, Biophys. J. 80 (2001) 643–655.
[24] J. Luneberg, I. Martin, F. Nubler, J.M. Ruysschaert, A. Hermann, J. Biol. Chem. 270 (1995) 27606–27614.
[25] S.A. Kamath, T.C. Wong, Biophys. J. 83 (2002) 135–143.
[26] L. Kale, R. Skeel, M. Bhandarkar, R. Brunner, A. Gursoy, N. Krawetz, J. Philips, A. Shinozaki, K. Varadarajan, K. Shulten, NAMD2, J. Comput. Phys. 151 (1999) 283–312.
[27] A.D. MacKerell Jr., D. Bashford, M. Bellott, R.L. Dunbrack Jr., J.D. Evanseck, M.J. Field, S. Fischer, J. Gao, H. Guo, S. Ha, D. Joseph-McCarthy, L. Kuchnir, K. Kuczera, F.T.K. Lau, C. Mattos, S. Michnick, T. Ngo, D.T. Nguyen, B. Prodhom, W.E. Reiher III, B. Roux, M. Schlenkrich, J.C. Smith, R. Stote, J. Straub, M. Watanabe, J. Wiorkiewicz-Kuczera, D. Yin, M.J. Karplus, J. Phys. Chem., B 102 (1998) 3586–3616.
[28] M. Schlenkrich, J. Brickmann, A.D. MacKerell Jr., M. Karplus, An empirical potential energy function for phospholipids, criteria for parameter optimization and applications, in: K.M. Merz, B. Roux (Eds.), Biological Membranes: A Molecular Perspective from Computation and Experiment, Birkhauser, 1996.
[29] T. Darden, D. York, L. Pederson, J. Chem. Phys. 98 (1993) 10089–10092.
[30] J.P. Ryckaert, G. Cicotti, H.J.C. Berendsen, J. Comput. Phys. 23 (1977) 327–341.
[31] S.E. Feller, Y. Zhang, R.W. Pastor, B.R. Brooks, J. Chem. Phys. 103 (1998) 4613–4621.
[32] A.D. MacKerell, J. Phys. Chem. 99 (1995) 1846–1854.
[33] M. Rafalski, J.D. Lear, W.F. DeGrado, Biochemistry 29 (1990) 7917–7922.
[34] I. Martin, Q.F. Defrise, V. Mandieau, N.M. Nielsen, T. Seermark, A. Burny, R. Brasseur, J.M. Ruysschaert, M. Vandenbranden, Biochem. Biophys. Res. Commun. 175 (1991) 872–879.
[35] L.M. Gordon, P.W. Mobley, R. Pilpa, M.A. Sherman, A.J. Waring, Biochim. Biophys. Acta 1559 (2002) 96–120.
[36] D.K. Chang, S.F. Cheng, W.J. Chien, J. Virol. 71 (1977) 6593–6602.
[37] I. Martin, M.C. Dubois, F. Defrise-Quertain, T. Saermark, A. Burny, R. Brasseur, J.M. Ruysschaert, J. Virol. 68 (1994) 1139–1148.
[38] G. Ravishanker, S. Vijaykumar, D.L. Beveridge, American Chemical Society, Washington, DC (1994) 209–219.
[39] J.P. Bradshaw, M.J.M. Darkes, T.A. Harroun, J. Katsaras, R.M. Epand, Biochemistry 39 (2000) 6581–6585.
[40] J.L. Nieva, S. Nir, A. Muga, F.M. Goni, J. Wilschut, Biochemistry 33 (1994) 3201–3209.

[41] L.M. Gordon, C.C. Curtain, Y.C. Zhong, A. Kirpatrick, P.W. Mobley, A.J. Waring, Biochim. Biophys. Acta 1139 (1992) 257–274.
[42] F.B. Pereira, F.M. Goni, A. Muga, J.L. Nieva, Biophys. J. 73 (1997) 1977–1986.
[43] S.E. Taylor, B. Desbat, D. Blaudez, S. Jacob, L.F. Chi, H. Fuchs, G. Schwarz, Biophys. Chem. 87 (2000) 63–72.
[44] R.M. Epand, Biochim. Biophys. Acta 1376 (1998) 353–368.
[45] R.W. Doms, J.P. Moore, J. Cell Biol. 151 (2000) F9–F13.
[46] D.M. Eckert, P.S. Kim, Proc. Natl. Acad. Sci. U. S. A. 98 (2001) 11187–11192.
[47] A. Saez-Cirion, J.L. Nieva, Biochim. Biophys. Acta 1564 (2002) 57–65.